

Anomalous coarsening and glassy dynamics

This article has been downloaded from IOPscience. Please scroll down to see the full text article.

2002 J. Phys.: Condens. Matter 14 1397

(<http://iopscience.iop.org/0953-8984/14/7/302>)

View [the table of contents for this issue](#), or go to the [journal homepage](#) for more

Download details:

IP Address: 171.66.16.27

The article was downloaded on 17/05/2010 at 06:09

Please note that [terms and conditions apply](#).

Anomalous coarsening and glassy dynamics

M R Evans

Department of Physics and Astronomy, University of Edinburgh, Mayfield Road,
Edinburgh EH9 3JZ, UK

E-mail: m.r.evans@ed.ac.uk

Received 18 December 2001

Published 7 February 2002

Online at stacks.iop.org/JPhysCM/14/1397

Abstract

An overview of the related topics of anomalous coarsening and glassy dynamics is given. In anomalous coarsening, the typical domain size of an ordered phase grows more slowly with time than the power law dependence that is usually observed, for example, in magnetic systems. We discuss how anomalous coarsening may arise through domain-size-dependent energy barriers in the coarsening process. We also review the phenomenology of glassy dynamics and discuss how simple nonequilibrium models may be used to reproduce certain aspects of the phenomenology. In particular, models involving dynamical constraints that give rise to anomalous coarsening are considered. Two models, the asymmetric constrained Ising chain and the ABC model, are discussed in detail with emphasis on how the large energy barriers to coarsening arise through the local dynamical constraints. Finally, the relevance of models exhibiting anomalous coarsening to glassy systems is discussed in a wider context.

1. Introduction

In this paper I shall review some very simple dynamical models whose dynamics slow down with time. Along with this, some typical length scale in the system grows. These two features are referred to as ‘glassy dynamics’ and ‘coarsening’ respectively. Anomalous coarsening refers to the situation where a length scale grows more slowly with time than the usual power law dependence. In this introduction I shall briefly review these topics and their interconnections. Then in the later sections I shall describe in detail two models that exhibit anomalous coarsening and glassy dynamics. The appealing feature of the models to be discussed is that although they exhibit nontrivial behaviour they are simple enough to analyse and gain a firm understanding of. In sections 2, 3 I shall summarize these analyses. Although the choice of models to be reviewed reflects personal research interests, I believe that the two models studied in sections 2 and 3 are each representative of a class of systems. To bring this out I try to make connections to other related models in sections 2.5 and 3.8. Finally, in section 4, I return to the relation between glassy dynamics and coarsening.

1.1. Glassy dynamics

The phenomenology of glassy systems is well established—see [1] for excellent reviews. Experimentally, the archetypal system is a liquid that, when cooled rapidly to temperatures where the equilibrium state should be a crystalline solid, becomes trapped in metastable liquid-like configurations. Thus the higher-temperature configurations are frozen in and one can meaningfully say that the glass is like a frozen liquid¹.

Three distinguishing features of the glassy state are the long relaxation times, stretched exponential decay of correlation functions (see equation (3) below) and ageing phenomena [2] whereby since the system is out of thermal equilibrium it evolves continuously as time goes by and time-translational invariance is lacking. This phenomenology provides a mandate for theoretical study.

The long relaxation times that show a non-Arrhenius divergence as the temperature T is lowered are often fitted experimentally by the Vogel–Tammann–Fulcher (VTF) law

$$\tau = \tau_0 \exp[-B/(T - T_0)]. \quad (1)$$

The relaxation time τ may characterize, for example, the time for an externally imposed stress to relax. Although some heuristic justifications have been offered [3], for practical purposes VTF is just a fit with three parameters τ_0 , B , T_0 . With $T_0 = 0$ it reduces to an Arrhenius law. A system for which T_0 is small, so that one has something close to Arrhenius behaviour, is referred to as a ‘strong glass’, whereas a system exhibiting large deviations from Arrhenius behaviour is referred to as a ‘fragile glass’. Generally, T_0 is much lower than the experimental temperatures so although there is a singularity in the fit, it is not physically relevant. Nevertheless it should be noted that there has been a long debate concerning whether T_0 represents a true thermodynamic transition temperature achievable in the limit of infinitely slow cooling.

On the other hand, other alternative functional forms for relaxation times $\tau(T)$ have been proposed that do not exhibit singularities at any finite T . Among these, the exponential inverse temperature squared (EITS) form

$$\tau \sim \exp(\text{const}/T^2) \quad (2)$$

(where the constant is positive) is popular. Experimentally, it is difficult to distinguish between VF and EITS behaviour due to obvious limitations on the longest accessible timescales; both can represent the experimentally observed $\tau(T)$ in many materials [4].

Stretched exponential decay of correlation functions, let us say an autocorrelation $q(t)$, is expressed by the Kohlrausch–Williams–Watt law

$$q(t) \sim \exp[-(t/\tau)^\theta] \quad (3)$$

where the stretching exponent $\theta < 1$. A heuristic explanation for this law is to postulate a broad distribution $\Omega(\tau)$ of relaxation modes with decay constants τ , yielding

$$q(t) = \int d\tau \Omega(\tau) \exp(-t/\tau). \quad (4)$$

If one assumes $\Omega(\tau) \sim \exp(-a\tau^\gamma)$ then for large t a poor man’s saddle point argument implies that the dominant modes have $\tau = (t/a\gamma)^{1/(\gamma+1)}$, which leads to (3) with $\theta = \gamma/(1 + \gamma)$. However the question remains as to how the broad distribution of modes $\Omega(\tau)$ comes about.

¹ Strictly one may distinguish between a supercooled liquid and a glass according to the rate of the cooling schedule but this issue is not pertinent here.

1.2. Kinetically constrained models

One idea that was proposed to generate a broad distribution of relaxation times was of a hierarchy of degrees of freedom [5]. The different levels in the hierarchy then relax in series, the degrees of freedom in one level having to wait for the degrees of freedom in the level above to reach some configuration before they are free to evolve. This latter condition is a realization of a *dynamical constraint*.

A more concrete realization of a dynamical constraint in a system with just one set of degrees of freedom is the n -spin facilitated kinetic Ising models introduced by Fredrickson and Anderson [6–8]. That model comprises noninteracting Ising spins in a downwards pointing field. However a spin can only flip if at least n nearest-neighbour spins are pointing up (against the field). This gives rise to slow cooperative relaxation. A modification of this model is to have anisotropic dynamical constraints [9–14]. In the one-dimensional version which we shall refer to as the asymmetric constrained Ising chain (ACIC) a spin can flip down only if its left neighbour is pointing up. As we shall show in section 2, although the equilibrium distribution is the Boltzmann distribution, the relaxation to equilibrium is strongly affected by the asymmetric constraint. Thus when quenching from high temperature to low temperature the equilibrium distribution implies that most spins should be pointing down. However for a spin to flip down its neighbour has to point up. Thus there is an energy barrier for isolated up-spins to flip down that is related to the size of the domains of down-spins separating these up-spins (this will be quantified in section 2). As the system gets closer to equilibrium these domains become longer and the energy barriers increase. Thus the dynamic slows down.

Dynamical constraints can also induce ‘entropy barriers’. In this case there are no energy barriers to relaxation, rather one can imagine special configurations or small doors in the phase space that the system must pass through to allow it to relax. These doors are found through random exploration of the phase space. However, as the relaxation proceeds the doors become progressively fewer and harder to find. One example of such a system is the Backgammon model [15].

Finally one should contrast the idea of energy (or free energy) barriers induced by dynamical constraints with energy barriers induced by disorder. It is well known that in a disordered system, where there is competition between different quenched random interactions, one can have large energy barriers in the phase space. It has been argued that such quenched disorder can mimic glassy systems (which are generally nondisordered). The theoretical machinery developed in the study of disordered systems then allows one to proceed in calculations [16]. However, one still has to come up with arguments that relate the quenched disorder to some dynamically ‘self-induced disorder’ [17, 18]. Alternatively one can go one step further and simply make assumptions about the phase space, such as a valley structure, without specifying how such features arise as a result of the microscopic model. This forms the basis of the ‘trap model’ [19, 20]. In that scenario one has a distribution of trap depths in the phase space. With increasing time the system will explore deeper and deeper traps and remain in them for longer and longer.

1.3. Coarsening

We now turn to the idea of coarsening and make comparisons with the glassy dynamics discussed so far. To visualize a coarsening system think of quenching a system from a high-temperature phase where its order parameter is zero to a low-temperature where the order parameter can take some number of nonzero values (each different value corresponding to a different ordered phase). Domains of the ordered phase(s) emerge and grow in time and it is

this phenomenon that is referred to as coarsening. At late times the system enters a *scaling regime*, that is a regime characterized by a single length scale (the typical size of domains) $\ell(t)$ that grows as $\ell(t) \sim t^n$. In this late-time scaling regime the distribution of domains, once scaled by $\ell(t)$, is statistically invariant. Thus the typical domain size indicates the age of the coarsening system. The value of the exponent n depends on the symmetry of the order parameter and conservation laws of the system. For a review see [22].

As a concrete example consider the zero-temperature Ising model with Glauber spin-flip dynamics (nonconserved order parameter). Domains of up-spins and down-spins are separated by domain walls that perform random walks: a step of the walk corresponds to the event that one of the spins adjacent to the domain wall flips. When two domain walls meet they annihilate and a domain is eliminated. Straight away one can argue roughly that, since the domain wall motion is diffusive, the time typically required to eliminate domains of size l is $T(l) \sim l^2$. Thus the typical domain size after time t is $\ell \sim t^{1/2}$.

More precisely one can write the growth law as a differential equation by noting that the rate of change of the typical domain size should be proportional to the inverse of the mean time to eliminate a domain multiplied by the size of the domain being eliminated

$$\frac{\partial \ell}{\partial t} \propto \frac{\ell}{T(\ell)} = \frac{1}{\ell} \quad (5)$$

and one recovers $\ell \sim t^{1/2}$. This growth exponent actually holds for a nonconserved scalar order parameter in two dimensions and above [22].

Now consider generalizing (5) to the case where some energy barrier ΔE (or more strictly free energy barrier) is involved in the elimination of the domains and the system is at low but finite temperature:

$$\frac{\partial \ell}{\partial t} \propto \frac{e^{-\Delta E/T}}{\ell}. \quad (6)$$

Actually this precludes one-dimensional systems that only order up to a finite length scale at finite temperature (see section 3), but at very low T one can consider the ordering process up to that finite length. Some possible scenarios resulting from (6) have been categorized in [21]. If the barriers ΔE are independent of ℓ one recovers $\ell \sim t^{1/2}$ growth. If the barriers are proportional to ℓ^m one obtains $\ell \sim [\ln t]^{1/m}$; in particular $m = 1$ yields logarithmic growth. In section 2 it will be shown that for the ACIC discussed in section 1.2 the energy barriers are logarithmic in ℓ thus yielding from (6) a growth law where the growth exponent is proportional to the temperature as $T \rightarrow 0$. In section 3 models will be discussed that have energy barriers that are linear in ℓ thus yielding domain growth that is logarithmic in time. For a particular model, the ABC model [23], it will be shown how these linear energy barriers arise. We refer to such cases where something different from power law growth with temperature-independent exponent is exhibited as *anomalous* coarsening.

A common approach in the study of coarsening is to make an approximation of a mean-field nature. That is, one focuses on the probability distribution of the domain sizes and ignores spatial correlations between domains. Such an approach is variously referred to as an interparticle distribution function [24], an independent interval approximation [25] or a ‘bag model’ [26]. To visualize this one thinks of placing all the domains in a bag, i.e. forgetting how domains are arranged with respect to one another. Then the dynamics become the updating of the domains in the bag. At each update a domain is selected from the bag along with temporary neighbours. An update rule is implemented that depends on the shape/size of the domain and its neighbours. After the update the domains are all replaced in the bag. For example, in models where domain walls diffuse and annihilate or coalesce, such as the kinetic Ising model discussed above, the update rule is to lengthen and shorten domains according to

how the domain wall moves. In another class of models [26, 27], domains are eliminated at each update with probabilities depending on their size; then the length of an eliminated domain is distributed amongst the neighbours.

1.4. Nonequilibrium steady states

So far, although we have discussed glassy systems out of thermal equilibrium, the dynamics have implicitly been assumed to obey detailed balance in the equilibrium state. Detailed balance means that in the steady state there is no net flow of probability between any two configurations. However one can consider a much larger class of nonequilibrium systems that are defined solely by their dynamics, without reference to any energy function. Although these systems may relax to some steady state it need not be a steady state described by Gibbs–Boltzmann statistical mechanics. In general there will be a net flow of probability between pairs of configurations, leading to probability current loops in the configuration space.

Examples of nonequilibrium steady states are given by driven systems with open boundaries where a mass current is driven through the system. Thus the system is driven by its environment rather than being in thermal equilibrium with its environment. In such a driven steady state generic long-range correlations may be exhibited [28]. This is in contrast to an equilibrium state which only exhibits long-range correlations at nongeneric points i.e. phase transitions. Since there is no energy function and Gibbs–Boltzmann statistical mechanics does not apply, there is no general formulation within which to solve for such a driven steady state. However it has often been suggested that the generic long-range correlations may result from some effective long-range Hamiltonian that could describe the dynamics.

Of particular interest have been one-dimensional nonequilibrium systems. For models respecting detailed balance it is well known that no phase transition or ordering process that continues indefinitely can occur. However for nonequilibrium systems this is not the case [29]. Thus nonequilibrium systems afford new possibilities for coarsening processes even in one-dimensional systems [30]. Moreover there are a number of exactly solvable one-dimensional nonequilibrium systems [31]. In section 3 the steady state of the ABC model will be solved for some special cases and it will be shown how strong phase separation along with anomalous coarsening can occur in one-dimensional systems.

2. Asymmetric constrained Ising chain

In this section I discuss the model introduced by Jäckle and Eisinger [9, 10]. As discussed in section 1.2 it was originally introduced as a model of cooperative, glassy relaxation. In particular the directed nature of the dynamical constraint implies a hierarchy in the spin relaxation. As I shall now describe the directed nature of the constraint also makes the model amenable to analysis.

2.1. Model definition

The model comprises L Ising spins $s_i = 0, 1$ on a one-dimensional lattice with periodic boundary conditions (site $i = L + 1$ is identified with site $i = 1$). The dynamics are defined by the following spin-flip rates:

$$\begin{aligned} 11 &\rightarrow 10 && \text{with rate } 1 \\ 10 &\rightarrow 11 && \text{with rate } \epsilon \end{aligned} \tag{7}$$

where

$$\epsilon = \exp(-1/T). \quad (8)$$

Thus a spin can only flip if its left neighbour is pointing up (note that in [9] the mirror image of the above definition was used, so that the right neighbour had to point up for a spin to be able to flip). By a rate, say x , we mean that in a small time dt the event happens with probability $x dt$. It is easy to check that the dynamics obey detailed balance with respect to an energy function $E = \sum_{i=1}^L s_i$, i.e. the equilibrium distribution corresponds to free spins in a downwards pointing field:

$$P_{\text{eq}}(\{s_i\}) = \frac{1}{Z} \exp\left[-\frac{\sum_i s_i}{T}\right] = \frac{\epsilon^{\sum_i s_i}}{(1+\epsilon)^L}. \quad (9)$$

It follows that the equilibrium concentration of up-spins, $c = \langle s_i \rangle$, is given by

$$c = \frac{\epsilon}{1+\epsilon}. \quad (10)$$

Although (9) would hold for a number of different dynamics obeying detailed balance, other properties such as two-time correlation functions may be sensitive to the particular choice of dynamics.

It is clear that the asymmetric dynamical constraint implies that information propagates to the right only. Thus in a thermodynamic limit where information cannot propagate all the way around the ring back to the starting point, we must have $\langle s_{i+k}(0)s_i(t) \rangle_{\text{eq}} - c^2 = 0$ for $k > 0$. However, the fact that detailed balance holds implies that in the steady state we must have reversibility. To see this note that when one has detailed balance there is no net flow of probability between any two configurations. Since there is no flow of probability there is nothing to distinguish the forwards direction in time from the backwards direction. Therefore running the systems backwards in time will not change any two-time correlation functions and

$$\langle s_{i+k}(0)s_i(t) \rangle_{\text{eq}} = \langle s_{i+k}(t)s_i(0) \rangle_{\text{eq}}. \quad (11)$$

Since we have argued that for $k > 0$ the left-hand side of (11) is equal to c^2 we deduce that the connected correlation function must be site diagonal:

$$\langle s_i(0)s_j(t) \rangle_{\text{eq}} - c^2 \propto \delta_{ij}. \quad (12)$$

This result is particular to the fully asymmetrically constrained model.

We shall be interested mainly in the behaviour after a quench from equilibrium at some high initial temperature $T \gg 1$ to low temperature $T \ll 1$ ($\epsilon \rightarrow 0$). At low temperatures the equilibrium concentration of up-spins (10) is small. Thus the quench is followed by a process of elimination of up-spins. However to eliminate an up-spin one first has to generate an adjacent up-spin. This implies energy barriers in the system's evolution. In figure 1 the sequence of events after such a quench is illustrated schematically.

The basic objects that we use for the description of the system are *domains*. As shown by the vertical lines in

$$\dots 1|0001|1|1|01|001|1|1|01|0\dots$$

a domain consists of an up-spin and all the down-spins that separate it from the nearest up-spin to the left. The length d of a domain then gives the distance between the up-spin at its right edge and the nearest up-spin to the left. Note that adjacent up-spins are counted as separate domains of length $d = 1$. In equilibrium, the distribution of domain lengths and its average are

$$P_{\text{eq}}(d) = \epsilon/(1+\epsilon)^d \quad d_{\text{eq}} = 1 + 1/\epsilon. \quad (13)$$

$$\begin{array}{rcl}
T \gg 1 & & 0110101110011 \\
& & \downarrow \\
T \ll 1 & & 0100101000010 \\
& & \downarrow \\
c \rightarrow \epsilon/(1+\epsilon) & & 0100000000010
\end{array}$$

Figure 1. Schematic representation of the evolution of the system following a deep quench. Before the quench $T \gg 1$ and c , the concentration of up-spins, $\simeq 1/2$. After the quench all the ‘mobile’ up-spins (i.e. those adjacent to other up-spins) are eliminated first. A slow coarsening process ensues that reduces the density of up-spins c to its equilibrium value.

Now consider what happens after a deep quench to $T \ll 1$, $\epsilon \ll 1$. The equilibrium concentration of up-spins at the final temperature T is $c = 1/d_{\text{eq}} = \epsilon + \mathcal{O}(\epsilon^2)$; hence the equilibrium probability of finding an up-spin within a chain segment of *finite* length d is $\mathcal{O}(d\epsilon)$ and tends to zero for $\epsilon \rightarrow 0$. In this limit ($\epsilon \rightarrow 0$ at fixed d), the flipping down of up-spins therefore becomes *irreversible* to leading order. In terms of domains, this means that the coarsening dynamics of the system is one of coalescence of domains: an up-spin that flips down merges two neighbouring domains into one large domain.

Such coarsening processes have been studied in a variety of contexts. In particular irreversible coarsening processes in which the rate of elimination depends solely on the domain size have a very convenient property: during such a process, no correlations between the lengths of neighbouring domains can build up if there are none in the initial state [27]. For the present model the equilibrated initial state consists of domains independently distributed according to (13) and is indeed uncorrelated. We take advantage of this property in section 2.3 to obtain an exact solution of the coarsening dynamics. We first discuss in detail how energy barriers arise in the dynamics.

2.2. Energy barriers

First we estimate the typical rate $\Gamma(d)$ at which domains of length d disappear by coalescing with their right neighbours. Because domain coalescence corresponds to the flipping down of up-spins, $\Gamma(d)$ can also be defined as follows. Consider an open spin chain of length d , with a ‘clamped’ up-spin ($s_0 = 1$) added on the left. Starting from the state $(s_0, s_1, \dots, s_d) = 10\dots 01$, $\Gamma^{-1}(d)$ is the typical time needed to reach the empty state $10\dots 00$ where spin s_d has ‘relaxed’ i.e. has flipped down. Any instance of this relaxation process can be thought of as a path connecting the initial and final states. Let us call the maximum number of ‘excited’ spins (up-spins except s_0) encountered along a path its height h . One might think that the relaxation of spin s_d needs to proceed via the state $11\dots 1$, giving a path of height d . In fact, the minimal path height $h(d)$ is much lower and given by

$$h(d) = n + 1 \quad \text{for } 2^{n-1} < d \leq 2^n \quad \text{where } n = 0, 1, \dots \quad (14)$$

To get a feeling for the result (14) consider in figure 2 some small domain sizes. The figure illustrates that to generate an up-spin adjacent to the right boundary spin of the domain one can proceed via a sequence of stepping-stones, for example for $d = 4$ one first generates an isolated up-spin in the middle of the domain then uses this stepping-stone to generate the subsequent excited spins in a similar manner to the relaxation of a $d = 2$ domain.

The result (14) is easily demonstrated for $d = 2^n$ [13]. To relax the 2^n th spin s_{2^n} , one can first flip up $s_{2^{n-1}}$ and use it as a stepping-stone for relaxing s_{2^n} . The corresponding path is

$d = 1$	$1\underline{1} \rightarrow 10$	$h(1) = 1$
$d = 2$	$101 \rightarrow 1\underline{11} \rightarrow 110 \rightarrow 100$	$h(2) = 2$
$d = 3$	$1001 \rightarrow 1101 \rightarrow 1\underline{111} \rightarrow \dots \rightarrow 1000$	$h(3) = 3$
$d = 4$	$10001 \rightarrow \dots \rightarrow 1\underline{1101} \rightarrow 10101 \rightarrow$ $10\underline{111} \rightarrow \dots \rightarrow 10100 \rightarrow \dots \rightarrow 10000$	$h(4) = 3$

Figure 2. Paths through spin configurations in the elimination of a domain of size d that traverse the minimum energy barrier. The height of the barrier is $h(d)$ and the highest-energy configuration(s) along the path has its excess excited spins underlined.

(with $s_{2^{n-1}}$ and s_{2^n} underlined)

$$1 \dots \underline{0} \dots \underline{1} \rightarrow 1 \dots \underline{1} \dots \underline{1} \rightarrow 1 \dots \underline{1} \dots \underline{0} \rightarrow 1 \dots \underline{0} \dots \underline{0} \quad (15)$$

and reaches height $h(2^n) = h(2^{n-1}) + 1$; the +1 arises because the stepping-stone stays up while the spin 2^{n-1} to its right is relaxed. Continuing recursively, one arrives at $h(2^n) = h(1) + n$; but $h(1) = 1$ because the only path for the relaxation of s_1 is $11 \rightarrow 10$. Thus we obtain equation (14) for $d = 2^n$; a proof for general integer d is given in [14].

From (14) it is evident that the energy barrier ΔE for the elimination of a domain of size d is $\Delta E \simeq \ln d / \ln 2$. Thus the rate at which such domains are eliminated is

$$\Gamma(d) \sim \epsilon^{(-\ln d / \ln 2)} = d^{-1/T \ln 2}.$$

From the discussion of section 1.3 and equation (5) we deduce that the typical domain size grows and the typical energy (number of up-spins) decreases as

$$d_{\text{typ}} \sim t^{T \ln 2} \quad E_{\text{typ}} \sim t^{-T \ln 2}. \quad (16)$$

Also since $d_{\text{eq}} \simeq \epsilon^{-1} = e^{1/T}$ the equilibration time is

$$t_{\text{eq}} \sim \exp[1/T^2 \ln 2]. \quad (17)$$

2.3. Hierarchical coarsening

From the scaling of $\Gamma(d)$, the coarsening dynamics in the limit $\epsilon \rightarrow 0$ naturally divides into stages distinguished by $n = h(d) - 1 = 0, 1, \dots$. During stage n , the domains with lengths $2^{n-1} < d \leq 2^n$ disappear; we call these the ‘active’ domains. This process takes place on a timescale of $\mathcal{O}(\Gamma^{-1}(d)) = \mathcal{O}(\epsilon^{-n})$; because the timescales for different stages differ by factors of $1/\epsilon$, we can treat them separately in the limit $\epsilon \rightarrow 0$. Thus during stage n active domains are eliminated and the distribution of inactive domains ($d > 2^n$) changes because elimination of an active domain implies coalescence with a neighbouring domain and results in the creation of a new inactive domain.

As discussed above for the irreversible system there are no correlations between neighbouring domains. Therefore we can work directly with the probability of domain sizes $P(d, t)$, i.e. the independent interval approximation sketched in section 1.3 is actually exact.

To examine stage n of the dynamics, where we assume that all domains with $d \leq 2^{n-1}$ have been eliminated, we shall rescale the time variable to $\tau = t\epsilon^n$. For the purpose of illustrating this procedure we write an approximate master equation for stage n

$$\frac{\partial}{\partial t} P(d, t) = -\Gamma(d)P(d, t) + \sum_{d'=2^{n-1}+1}^{\infty} \Gamma(d')P(d', t)P(d-d', t). \quad (18)$$

The first term in the right-hand side of (18) represents domains of size d being eliminated; the second term represents the domains of size d being created through a domain of size d' coalescing with a domain of size $d - d'$. The equation is approximate because the elimination of a domain is a complex process that cannot be represented by a single rate; however, the exact result will be obtained when time is rescaled (see [14] for a presentation that avoids the inexactitude of (18)). We introduce rescaled time by defining $\tau = t\epsilon^n$; during stage n of the dynamics and in the limit $\epsilon \rightarrow 0$, it can take on any positive value $\tau > 0$. Defining $\tilde{\Gamma}(d) = \Gamma(d)/\epsilon^n$ and taking the limit $\epsilon \rightarrow 0$ the master equation reduces to

$$\text{for } 2^n \geq d > 2^{n-1} \quad \frac{\partial}{\partial \tau} P(d, \tau) = -\tilde{\Gamma}(d)P(d, \tau) \quad (19)$$

$$\text{for } d > 2^n \quad \frac{\partial}{\partial \tau} P(d, \tau) = \sum_{d'=2^{n-1}+1}^{2^n} \tilde{\Gamma}(d')P(d', \tau)P(d-d', \tau). \quad (20)$$

To proceed we define the generating function

$$G(z, \tau) = \sum_{d=2^{n-1}+1}^{\infty} P(d, \tau)z^d \quad (21)$$

and its analogue for the active domains,

$$H(z, \tau) = \sum_{d=2^{n-1}+1}^{2^n} P(d, \tau)z^d. \quad (22)$$

Then multiplying (19), (20) by z^d and summing appropriately yields

$$\frac{\partial}{\partial \tau} H(z, \tau) = - \sum_{d=2^{n-1}+1}^{2^n} \tilde{\Gamma}(d)P(d, \tau)z^d \quad (23)$$

$$\begin{aligned} \frac{\partial}{\partial \tau} G(z, \tau) &= \frac{\partial}{\partial \tau} H(z, \tau) + \sum_{d=2^{n+1}}^{\infty} \sum_{d'=2^{n-1}+1}^{2^n} \tilde{\Gamma}(d')P(d', \tau)P(d-d', \tau)z^d \\ &= \left(\frac{\partial}{\partial \tau} H(d, \tau) \right) [1 - G(z, \tau)] \end{aligned} \quad (24)$$

(where the last equality follows by reordering the sums over d and d'). Equation (24) may be integrated and one obtains

$$\frac{1 - G(z, \tau)}{1 - G(z, 0)} = \exp(-[H(z, \tau) - H(z, 0)]). \quad (25)$$

Now at the end of stage n , all domains that were active during that stage have disappeared, and so $H(z, \infty) = 0$. Thus

$$G(z, \infty) - 1 = [G(z, 0) - 1] \exp[H(z, 0)]. \quad (26)$$

Recall that we are considering stage n of the dynamics. The initial condition for stage $n + 1$ of the dynamics will be given by the distribution $P(d, t)$ at the end of stage n . Thus defining $G_n \equiv G(z, 0)$ for stage n , with a similar definition for the active generating function H_n , we can relate the different stages of the dynamics through

$$G_{n+1}(z) - 1 = [G_n(z) - 1] \exp[H_n(z)]. \quad (27)$$

This exact result relates, through their generating functions, $P_n(d)$ and $P_{n+1}(d)$, which are defined as the domain length distributions at the end of stages $n - 1$ and n of the dynamics respectively. Iterating it from a given initial distribution $P_0(d)$ gives $P_n(d)$ for all $n = 1, 2, \dots$

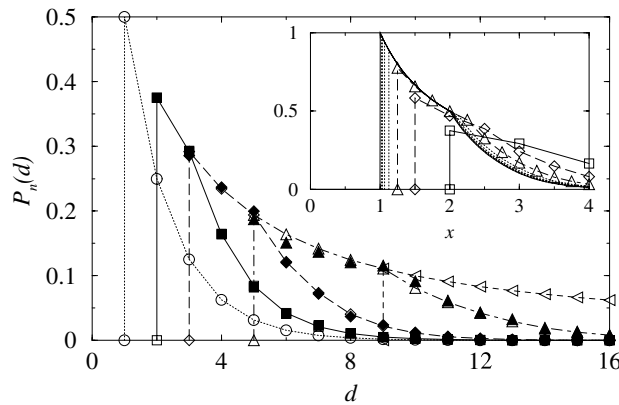


Figure 3. Domain length distributions $P_n(d)$ at the end of stage $n - 1$ of the low- T coarsening dynamics, for initial temperature $T = \infty$. Open symbols and curves: theoretical results, calculated from (27), for $n = 0$ (circles; initial condition), 1 (squares), 2 (diamonds), 3 (triangles). Full symbols: simulation results for a chain of length $L = 2^{15}$ and $\epsilon = 10^{-4}$ ($n = 1, 2$) and $\epsilon = 10^{-3}$ ($n = 3$). Inset: scaled predictions $2^{n-1}P_n(d = 2^{n-1}x)$ versus x for $n = 1, \dots, 8$. Bold curve: predicted scaling function (33) (figure taken from [14]).

Figure 3 shows numerical results for the case where $P_0(d)$ is the equilibrium distribution (13) corresponding to an initial temperature of $T = \infty$. It is clear that a scaling limit emerges for large n . By this it is meant that rescaled distributions

$$\tilde{P}_n(x) = 2^{n-1}P_n(d) \quad \text{where} \quad x = \frac{d}{2^{n-1}} \tag{28}$$

converge to a limiting distribution $\tilde{P}(x)$ for the scaled domain size x . This is just a statement of the invariance of the coarsening processes in each stage once the domain sizes are rescaled by the characteristic size domain size 2^{n-1} .

The change to a continuous variable x for the domain lengths simply results in generating functions $G(z, \tau)$, $H(z, \tau)$ being replaced by Laplace transforms. Invariance under (27) then gives the equation

$$g(2s) - 1 = [g(s) - 1] \exp[h(s)] \tag{29}$$

where

$$g(s, \tau) = \int_1^\infty dx \tilde{P}(x) e^{-sx} \quad h(s, \tau) = \int_1^2 dx \tilde{P}(x) e^{-sx}. \tag{30}$$

We found a solution to this equation by noting that the numerics strongly suggest $\tilde{P}(x) = 1/x$ for $1 < x < 2$. Using this as an ansatz implies

$$h(x) = \text{Ei}(s) - \text{Ei}(2s) \quad \text{where} \quad \text{Ei}(s) = \int_s^\infty \frac{e^{-u}}{u} du$$

which when inserted into (29) yields

$$[1 - g(s)] \exp(\text{Ei}(s)) = \text{constant}. \tag{31}$$

The requirement that $g(s) \rightarrow 0$ for large s fixes the constant as unity, which yields

$$g(s) = 1 - \exp(-\text{Ei}(s)). \tag{32}$$

Expanding the exponential as a series allows the Laplace transform to be inverted term by term and one obtains

$$\begin{aligned}
 \tilde{P}(x) &= \frac{1}{2\pi i} \int_{\gamma-i\infty}^{\gamma+i\infty} e^{sx} g(s) \\
 &= \frac{1}{2\pi i} \int_{\gamma-i\infty}^{\gamma+i\infty} e^{sx} \sum_{m=1}^{\infty} (-1)^{m+1} \frac{Ei^m}{m!} \\
 &= \sum_{m=1}^{\infty} \frac{(-1)^{m+1}}{m!} \int_1^{\infty} \prod_{r=1}^m \frac{dx_r}{x_r} \delta\left(\sum_{s=1}^m x_s - x\right) \\
 &= \Theta(x-1) \frac{1}{x} - \Theta(x-2) \frac{\ln(x-1)}{x} + \dots
 \end{aligned} \tag{33}$$

where $\Theta(x)$ is the Heaviside step function. This series (33) has singularities in the k th derivative at the integer values $x = k + 1, k + 2, \dots$.

It is interesting to note that $\tilde{P}(x)$ given by (33) is identical to the scaling function obtained for a simple ‘paste-all’ model of coarsening wherein the smallest domain on a one-dimensional lattice is eliminated by pasting it onto one of its neighbours [26].

The calculated $\tilde{P}(x)$ agrees well with the results obtained by direct iteration of (27) (figure 3). The average domain length in the scaling limit is given by $\bar{d}_n = 2^{n-1}\bar{x}$; from the results for $\tilde{P}(x)$ we find $\bar{x} = \exp(\gamma) = 1.78\dots$, where γ is Euler’s constant.

2.4. Stretched exponential relaxation

The result (17) for the EITS equilibration time $t_{\text{eq}} = \exp(1/T^2 \ln 2)$ is based on the extrapolation of the finite- \bar{d} coarsening behaviour, $\bar{d} \sim t^{T \ln 2}$, into the equilibrium region $\bar{d} = d_{\text{eq}} = \mathcal{O}(1/\epsilon)$, where it is no longer strictly valid. We now show, however, that the same timescale is obtained from the initial decay of the spin–spin autocorrelation function defined by

$$R(t) = \frac{\langle s_i(0)s_i(t) \rangle_{\text{eq}}}{\langle s_i(0) \rangle_{\text{eq}}} \tag{34}$$

at equilibrium at low temperature T .

In equation (34) $R(t)$ is the probability that an up-spin at $t = 0$ is also up at a later time t . As t increases, $R(t)$ decays from 1 to the equilibrium concentration of up-spins, $c = \epsilon/(1 + \epsilon)$. To find the initial decay of $R(t)$, consider the early stages of the dynamics (i.e. $t = \mathcal{O}(\epsilon^{-\nu})$ with ν finite). For $\nu \rightarrow n+$, all domains of length $d \leq 2^n$ will have disappeared because $t \gg \Gamma^{-1}(d)$. Therefore only up-spins that bounded longer domains at $t = 0$ will have an $\mathcal{O}(1)$ probability of still being up. From the equilibrium distribution (13), one sees that they constitute a fraction $(1 + \epsilon)^{-2^n}$ of the up-spins at $t = 0$, hence $R(\nu = n + 0) \simeq 1 - 2^n \epsilon + \mathcal{O}(\epsilon^2)$. Neglecting corrections of $\mathcal{O}(\epsilon^2)$, the quantity $-\ln R(\nu)$ thus lies between $2^{\nu-1}\epsilon$ and $2^\nu \epsilon$ (for $\nu > 0$).

Reverting to unscaled time t , we have

$$1/2 \leq -[\ln R(t)]/(t/t_{\text{eq}})^{T \ln 2} \leq 1 \tag{35}$$

for short times $(t/t_{\text{eq}})^{T \ln 2} \ll 1$, which implies

$$R \simeq \exp -[a(t/t_{\text{eq}})^{T \ln 2}] \tag{36}$$

i.e. stretched exponential relaxation with a stretching exponent that depends linearly on T . However this argument only holds strictly for $(t/t_{\text{eq}})^{T \ln 2} \ll 1$. For longer times the stretched exponential behaviour no longer holds and one requires a more sophisticated analysis [32].

Note that the timescale t_{eq} that enters here is the same as the equilibration time $t_{\text{eq}} = \exp(1/T^2 \ln 2)$ found above. Thus *to leading order* we can identify the equilibration time for coarsening after a quench with the equilibrium relaxation time; both have an EITS-divergence at low T . However the corrections to the EITS-divergence for the two timescales (e.g. factors of the form $\exp(a/T)$) need not be equal.

2.5. Other related models

Recently it has been shown that the coarsening theory described above for ACIC is also relevant to a three-spin interaction Ising model on a triangular lattice [33]. There a dual model entails the elimination of defects (corresponding to up-spins in the ACIC), subject to dynamical constraints. An EITS relaxation time is obtained and the independent interval approximation described here (exact for ACIC) can be used as a good approximation to the coarsening dynamics (see [54]).

One can also interpolate between the asymmetric constrained model and the symmetric constrained model [6] by introducing a parameter b into the dynamics [34]. The spin-flip rates are

$$\begin{array}{ccc}
 & 1-b & \\
 1 & 1 \xleftrightarrow{\quad} & 1 & 0 \\
 & (1-b)\epsilon & \\
 & b & \\
 1 & 1 \xleftrightarrow{\quad} & 0 & 1 \\
 & b\epsilon &
 \end{array} \tag{37}$$

The ACIC is recovered when $b = 0$ and the symmetric model is recovered when $b = 1/2$. In the symmetric model an isolated up-spin can effectively diffuse by creating a neighbouring up-spin then flipping down the original up-spin. The domain coalescence happens through this diffusion process. Thus the energy barrier for elimination of domains does not depend on domain size. This implies an Arrhenius relaxation law and ‘strong’ glass behaviour. The crossover to the ‘fragile’ glass behaviour seen for the ACIC (i.e. EITS relaxation time) as one varies the parameter b has been studied (see [55]).

Finally let us mention a constrained Ising spin chain where the field is induced dynamically [35]. The allowed spin flips have rates defined as follows:

$$\begin{array}{ccc}
 & 1/2 & \\
 0 & 1 & 1 \xleftrightarrow{\quad} & 0 & 0 & 1 \\
 & 1/2 & \\
 1 & 1 & 0 \xleftrightarrow{\quad} & 1 & 0 & 0 \\
 & 1/2 & \\
 0 & 1 & 0 \xrightarrow{\quad} & 0 & 0 & 0.
 \end{array} \tag{38}$$

Thus a down-spin inside an up-spin domain cannot flip up but an up-spin inside a down-spin domain can flip down. The domains of up-spins grow as normal as $t^{1/2}$ but the down-spin domains grow slightly more quickly as $t^{1/2} \ln t$. Eventually this results in a slow decay of the magnetization (number of up-spins as) $c \sim 1/\ln t$.

3. The ABC model

3.1. Coarsening in one-dimensional systems

First let us review why indefinite coarsening does not occur in equilibrium systems in one dimension. Perhaps the best known argument is that of Landau and Lifshitz [36]. (Other

arguments are summarized in [30].) For simplicity, consider a one-dimensional lattice of L sites with two possible states, say A and B, for each site variable. Let us assume the ordered phases, where all sites take state A or all sites take state B, have the lowest energy, and assume a domain wall (a bond on the lattice which divides a region of A phase from that of B) costs a finite amount of energy ϵ . Then n domain walls will cost energy $n\epsilon$ but the entropic contribution to the free energy due to the number of ways of placing n walls on L sites is $\simeq nT [\ln(n/L) - 1]$ for $1 \ll n \ll L$. Thus for any finite temperature a balance between energy and entropy ensures that the number of domain walls grows until it scales as L , that is, until the typical ordered domain size is finite.

Note that this argument relies on a finite energy cost for domain walls, and short-range interactions so that one may ignore the interaction energy of domain walls. If the domain walls can feel each other through some long-range mechanism then coarsening can ensue [37]. Also, of course, we require nonzero temperature so that entropy comes into play. In contrast, at zero temperature the one-dimensional kinetic Ising model discussed in the introduction does coarsen.

In the following we shall discuss a one-dimensional model where although the dynamics are local the system coarsens. In a special case one can understand this through the existence of an effective long-range energy function.

3.2. Model definition

Here we define a model, to be referred to as the ABC model, that exhibits phase separation in one dimension. Consider a one-dimensional periodic lattice of length N where each site is occupied by one of the three types of particle, A, B or C. The model evolves under a random sequential update procedure which is defined as follows: at each time step a pair of neighbouring sites is chosen randomly and the particles at these sites are exchanged according to the following rates:



The particles thus diffuse asymmetrically around the ring. The dynamics conserve the number of particles N_A , N_B and N_C of the three species.

The $q = 1$ case is special. Here the diffusion is symmetric and every local exchange of particles takes place with the same rate as the reverse move. The system trivially obeys detailed balance reaching a steady state in which all microscopic configurations (compatible with the number of particles N_A , N_B and N_C) are equally probable. This state is disordered and homogeneous; no phase separation takes place.

Now consider the case $q < 1$ (the case $q > 1$ can easily be understood by symmetry). As a result of the bias in the exchange rates an A particle moves preferentially to the left inside a B domain and to the right inside a C domain. Similarly the motion of B and C particles in foreign domains is biased. Consider the dynamics starting from a random initial configuration, figure 4(a). The configuration is composed of a random sequence of domains of A, B and C particles. Due to the bias a local configuration in which an A domain is placed to the right of a B domain is unstable and the two domains exchange places on a relatively short timescale

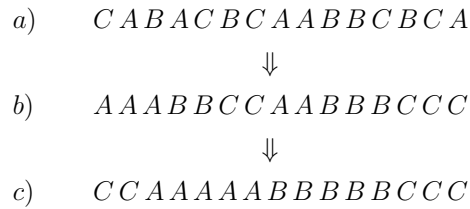


Figure 4. Schematic representation of the evolution of the system starting from a random initial condition (a). Initially all unstable domain walls (B A, C B or A C) are removed and one arrives at a metastable state (b). A slow coarsening process ensues in which the smallest domains are eliminated until one arrives at a fully phase-separated state (c), compare with figure 1.

which is linear in the domain size. Similarly, AC and CB domains are unstable too. On the other hand AB, BC and CA configurations are stable and long lived. Thus after a relatively short time the system reaches a state of the type illustrated in figure 4(b), in which A, B and C domains are located to the right of C, A and B domains, respectively. The evolution of this state takes place via a slow diffusion process in which, for example, A particles have to diffuse against a drift over an adjacent B domain. The timescale for an A particle to cross is $\propto q^{-l}$, where l is the size of the B domain. We use the discussion of section 1.3 and equation (5) to deduce that the system coarsens with an average domain size that increases with time as $\ln t / |\ln q|$. Eventually the system phase separates into three domains of the three species of the form $A \dots AB \dots BC \dots C$.

In a finite system the phase-separated state may further evolve and become disordered due to fluctuations. However, the timescale for this to happen grows exponentially with the system size. For example it would take a time of order of $q^{-\min\{N_B, N_C\}}$ for the A domain in the totally phase-separated state to break up into smaller domains. Hence in the thermodynamic limit, this timescale diverges and the phase-separated state remains stable provided the density of each species is nonzero. Note that there are always small fluctuations about a totally phase-separated state. However, these fluctuations affect the densities only near the domain boundaries. They result in a finite width for the domain walls (the density profile is not a step function but is smeared out like a Fermi function). The fact that any phase-separated state is stable for a time exponentially long in the system size amounts to a breaking of the translational symmetry, i.e. there are N equivalent ground states but the system has to spontaneously choose one of them.

Since the exchange rates are asymmetric, the system generically supports a particle current in the steady state, which implies that detailed balance does not hold. To see this, consider the A domain in the phase-separated state. An A particle near the $\dots AB \dots$ boundary can traverse the entire B domain to the right with an effective rate proportional to q^{N_B} . Once it crosses the B domain it will move through the C domain with speed $1 - q$. Similarly an A particle near the $\dots CA \dots$ boundary can traverse the entire C domain to the left with an effective rate proportional to q^{N_C} . Once the domain is crossed it moves through the B domain with speed $1 - q$. Hence the net A particle current is of the order of $q^{N_B} - q^{N_C}$. Since this current is exponentially small in system size, it vanishes in the thermodynamic limit. For the case of $N_A = N_B = N_C$, this argument suggests that the current is strictly zero for any N .

The arguments presented above suggesting phase separation for $q < 1$ may be easily extended to $q > 1$. In this case, however, the phase-separated state is BAC rather than ABC. This may be seen by noting that the dynamical rules are invariant under the transformation $q \rightarrow 1/q$ together with $A \leftrightarrow B$.

3.3. Special case $N_A = N_B = N_C$

The general argument presented in the previous subsection suggests that for the special case $N_A = N_B = N_C$, in the steady state (i.e. after the coarsening process), there are no currents for any system size. We demonstrate this explicitly by showing that the *local dynamics* of the model satisfies detailed balance with respect to a *long-range asymmetric* energy function \mathcal{H} .

We define the occupation variables as follows:

$$A_i = \begin{cases} 1 & \text{if site } i \text{ is occupied by an A particle} \\ 0 & \text{otherwise.} \end{cases} \quad (40)$$

The variables B_i and C_i are defined similarly. Clearly the relation $A_i + B_i + C_i = 1$ is satisfied. It turns out that for the case $N_A = N_B = N_C = N/3$ the steady-state distribution $W_N(\{X_i\})$ corresponding to the dynamics (39) may be written in terms of an energy function \mathcal{H} :

$$W_N(\{X_i\}) = Z_N^{-1} q^{\mathcal{H}(\{X_i\})} \quad (41)$$

$$\mathcal{H}(\{X_i\}) = \sum_{i=1}^{N-1} \sum_{j=i+1}^N [C_i B_j + A_i C_j + B_i A_j] - (N/3)^2. \quad (42)$$

Here Z_N is the partition sum given by $\sum q^{\mathcal{H}(\{X_i\})}$, where the sum is over all configurations in which $N_A = N_B = N_C$. Note that although the system is periodic and site 1 is not in any way special (42) appears to single out site 1. Thus it is not clear that (42) is translationally invariant under relabelling of the spins.

In order to turn equation (41) into a usual Boltzmann form one could define q as a temperature variable with

$$kT = -1/\ln q. \quad (43)$$

Thus, $q \rightarrow 1$ is the infinite-temperature limit, corresponding to the disordered state where each configuration is equally likely. The proof of equations (41), (42) is straightforward. This is done by considering a nearest-neighbour particle exchange and verifying that detailed balance is satisfied with respect to (39). Then we just have to check that the energy function is translationally invariant. We defer the proof to section 3.7, where we consider a more general m -species model.

Before proceeding further to evaluate the partition sum associated with the energy function (42) let us make a few observations. The ground state of the energy function is given by the fully separated state $A \dots AB \dots BC \dots C$ and its translationally related states. It is easy to check that the ground state with the A domain beginning at site 1 has zero energy since the contribution to the sum in (42) (coming from the $A_i C_j$ term) is equal to $(N/3)^2$. A simple way of evaluating the energy of an arbitrary configuration is obtained by noting that nearest-neighbour exchanges $AB \rightarrow BA$, $BC \rightarrow CB$ and $CA \rightarrow AC$ cost one unit of energy each while the reverse exchanges result in an energy gain of one unit. The energy of an arbitrary configuration may thus be evaluated by starting with the ground state and performing nearest-neighbour exchanges until the configuration is reached, keeping track of the energy changes at each step of the way. The highest energy is $N^2/9$ and it corresponds to the totally phase-separated configuration $A \dots AC \dots CB \dots B$ and its N translations. Note that the majority of configurations have energy proportional to N^2 . In section 3.4 it will be shown that this implies that only the ground states and low-energy excitations about them contribute to the equilibrium state.

$A \dots AB \dots BC \dots CAB CABC \dots ABC$

Figure 5. Metastable state that has the lowest energy for a given number s of domains of each species. The $3(s-1)$ rightmost domains are of size 1 and the three leftmost domains are of size $(N/3 - s + 1)$ each.

To write \mathcal{H} in a manifestly translationally invariant form we define $\mathcal{H}_{i_0}(\{X_i\})$ as the energy function in which site i_0 is the origin. Namely,

$$\mathcal{H}_{i_0}(\{X_i\}) = \sum_{i=i_0}^{N+i_0-2} \sum_{j=i+1}^{N+i_0-1} [C_i B_j + A_i C_j + B_i A_j] - (N/3)^2 \quad (44)$$

where the summation over i and j is modulo N . Summing (44) over all i_0 and dividing by N , one obtains

$$\mathcal{H}(\{X_i\}) = \sum_{i=1}^N \sum_{k=1}^{N-1} \left(1 - \frac{k}{N}\right) (C_i B_{i+k} + A_i C_{i+k} + B_i A_{i+k}) - (N/3)^2 \quad (45)$$

where in the summation the value of the site index $(i+k)$ is modulo N . In the energy function (45) the interaction is linear in the distance between the particles, and thus is long ranged. The distance is measured in a preferred direction from site i to site $i+k$. Thus the interaction is asymmetric.

3.4. Ground states and metastable states

A minimum of the energy (42) is realized by a configuration with no unstable domain walls (B A, C B or A C) so that any exchange of nearest-neighbour particles results in an increase in the energy. As well as the N ground states there are many metastable states. Any metastable state is composed of a sequence of domains separated by AB, BC and CA domain walls i.e. A, B and C domains follow C, A and B domains, respectively (see figure 4(b)). Therefore each metastable state has an equal number of domains of each type. We shall refer to any metastable state with s domains of each type, with $s = 1, \dots, N/3$, as an s -state; the total number of domains in an s -state is $3s$. The $s = 1$ case corresponds to the ground state while $s = N/3$ corresponds to the ABCABC...ABC state, composed of a total of N domains each of length 1. Note that in general the domains of an s -state need not be of equal length.

In the coarsening process it is these metastable states that control the dynamics. We discuss here some properties of the states such as their number and energy.

To obtain a bound for $\mathcal{N}(s)$, the number of metastable states with s domains of each species, note that the number of ways of dividing $N/3$ A particles into s domains is $\binom{N/3-1}{s-1}$. The number of ways of combining s divisions of each of the three types of particle is clearly $\left[\binom{N/3-1}{s-1}\right]^3$. There are at most N ways of placing this string of domains on a lattice to obtain a metastable state (the number of ways need not be equal to N since the string may possess some translational symmetry). One therefore has

$$\left[\binom{N/3-1}{s-1}\right]^3 \leq \mathcal{N}(s) \leq N \left[\binom{N/3-1}{s-1}\right]^3. \quad (46)$$

Thus, the total number of metastable states is exponential in N .

We now consider the energy of the metastable states. It is easy to convince oneself that among all s -states, none has energy lower than the configuration illustrated in figure 5.

The energy of this state, E_s , satisfies the following recursion relation:

$$E_{s+1} = E_s + N/3 - s \quad (47)$$

$$\underline{A} A \cdots A \underline{A B A B A B} B \cdots B \underline{B C C} C \cdots C \underline{C}$$

Figure 6. Excitation about a ground state at the A B domain wall of energy $E = 3$: one A particle has penetrated two exchanges into the B domain and a second A particle one exchange. This corresponds to the partition $3 = 2 + 1$. The domain wall regions are underlined.

with $E_1 = 0$. To see this from figure 5, note that the $s + 1$ -state may be created from the s -state by first moving a B particle from the leftmost B domain across $(N/3 - s)$ C particles to the right, costing $(N/3 - s)$ units of energy. Then move an A particle from the leftmost A domain to the right across the adjacent B and C domains; no net energy change results. Thus the total energy cost of the moves is $(N/3 - s)$, yielding (47). The recursion relation (47), together with $E_1 = 0$, is readily solved to give

$$E_s = (s - 1) \frac{N}{3} - \frac{s(s - 1)}{2}. \quad (48)$$

The energy of all metastable s -states is larger than or equal to E_s as given by equation (48). Note that E_s increases with s . Furthermore, for finite s the energy is linear in N whereas for $s \propto N$ the energy becomes quadratic in N .

Now let us consider the contribution of the metastable states to the partition sum. Multiplying the upper bound on the number of s -states (46) with the lower bound on the energy (48) one obtains an upper bound on the contribution to the partition sum that vanishes in the thermodynamic limit

$$N \left[\binom{N/3 - 1}{s - 1} \right]^3 q^{(s-1)N/3 - s(s-1)/2} \rightarrow 0 \quad \text{for } s > 1, q < 1 \text{ and } N \rightarrow \infty. \quad (49)$$

However, the contribution from the ground states $s = 1$ is N . Thus even though metastable states dominate the dynamics, they do not contribute to the partition sum since in (49) the energy grows more strongly than the entropic contribution.

3.5. Partition sum

We now analyse in more detail the behaviour of the partition sum. In principle one wants to compute

$$Z_N = \sum q^{\mathcal{H}(\{X_i\})} \quad (50)$$

where the sum is over *all* configurations in which $N_A = N_B = N_C$. First note that any configuration that contains unstable domain walls (i.e. is not a metastable state) can be associated with a metastable state by a path of decreasing energy comprising nearest-neighbour exchange eliminating of the unstable walls. Conversely the sum over all configurations may be implemented by summing over all ground states and metastable states and the excitations about those states. It is not hard to believe that as the metastable states make vanishing contributions to Z_N so do excitations about them. This is proven rigorously in [23]. In the following we just consider the excitations about the ground states. Consider figure 6, where a low-energy excitation about a ground state is illustrated. The excitation is localized near the A B domain wall and comprises one or more A particles penetrating into the B domain (equivalently B particles penetrating into the A domain). The energy cost is given by the sum of the distances each A particle has penetrated into the B domain. Thus the total number of excitations of energy m at the boundary is the number of ways of dividing m into an ordered set of integers corresponding to the distance the first A has moved, the distance the second A has moved and so on. This is equal to $P(m)$, the number of *partitions* of the integer m .

Several results concerning partitions are known [38]. First the generating function of $P(m)$ is given by

$$\sum_{m=0}^{\infty} q^m P(m) = \frac{1}{(q)_{\infty}} \quad (51)$$

$$\text{where } (q)_{\infty} = \lim_{n \rightarrow \infty} (1-q)(1-q^2) \cdots (1-q^n). \quad (52)$$

Although a simple explicit formula for $P(m)$ does not exist the asymptotic behaviour is given by

$$P(m) \simeq \frac{1}{4m\sqrt{3}} \exp(\pi(2/3)^{1/2} m^{1/2}). \quad (53)$$

Note that the increase is a stretched exponential in m , i.e. slower than exponential.

In the thermodynamic limit one can use (51) directly to calculate the sum of excitations around a domain wall, i.e. the sum over m of q^m , the weight of an excitation of energy m , multiplied by $P(m)$, the number of such excitations. For a finite system there should be some upper limit on m —for example, an A particle moved across the B domain will eventually reach the C domain—but this upper limit can be safely taken to infinity for large N [23]. By the same token the three domain walls have no significant interaction. Then one has that in the large- N limit and for all $q < 1$, the partition sum is given by

$$Z_N = N/[(q)_{\infty}]^3. \quad (54)$$

Here the factor N is a result of the sum of contributions from the N ground states and the cubic power comes from the product of excitations at the three domain walls.

Note that the partition sum is linear and not exponential in N , meaning that the free energy is not extensive. This reflects the fact that excitations are localized near the domain walls. In turn this stems from the fact that the energies of most configurations are $\mathcal{O}(N^2)$, which is a result of the long-range interaction in the energy function.

A consequence of this is that in the steady state the system is fully phase separated; that is, each of the domains is pure. This was demonstrated in [23] by showing that

$$\langle A_i A_{i+r} \rangle = \frac{1}{3} - \mathcal{O}(r/N) \quad (55)$$

for any given r and sufficiently large N . Thus the probability of finding a particle a large distance inside a domain of particles of another type is vanishingly small in the thermodynamic limit.

For q close to 1, $(q)_{\infty}$ as defined in (52), has an essential singularity

$$(q)_{\infty} = \exp \left\{ -\frac{1}{\ln q} [\pi^2/6 + \mathcal{O}(1-q)] \right\}. \quad (56)$$

This suggests that extensivity of the free energy could be restored in the double limit $q \rightarrow 1$ and $N \rightarrow \infty$ with $N \ln q$ finite. Physically one can understand this scaling variable as the ratio of the domain length ($N/3$) to the domain wall width ($\sim \int l q^l dl / \int q^l dl = 1/|\ln q|$). The validity of $N \ln q$ as a scaling variable was investigated in [23], where a good scaling collapse was obtained for the two-point correlation functions.

3.6. Coarsening

The analytic results of the previous subsection for $N_A = N_B = N_C$ give proof of the coarsening into three pure domains in that special case. Clearly one expects the same behaviour in the general case but to demonstrate it numerically requires prohibitively long timescales. In order

to study anomalously slow coarsening dynamics numerically one can employ an effective or toy model that may be more easily simulated. In this section I shall outline how this can be implemented.

We consider a system at time t such that the average domain size, $\langle l \rangle$, is much larger than the domain wall width. At these timescales, the domain walls can be taken as sharp and we may consider only events which modify the size of domains. This means that the dynamics of the system can be approximated by considering only the movement of particles between neighbouring domains of the same species. Thus only metastable states are considered in the toy model.

We represent a configuration by a sequence of integers of the form $a_1 b_1 c_1 a_2 b_2 c_2 \dots a_3 b_3 c_3$, where, for example, the i th domain of A particles is of length a_i . At each time step a pair of neighbouring domains of the same species of particle, say a_i and a_{i+1} , is chosen randomly. The exchange of particles between domains takes place at a rate dictated by the size of the domains b_i and c_i which separate them. Thus the lengths of the chosen domains are modified by carrying out one of the following processes:

$$\begin{aligned} (1) \quad & \left. \begin{array}{l} a_i \rightarrow a_i - 1 \\ a_{i+1} \rightarrow a_{i+1} + 1 \end{array} \right\} \text{ with rate } q^{b_i} \\ (2) \quad & \left. \begin{array}{l} a_i \rightarrow a_i + 1 \\ a_{i+1} \rightarrow a_{i+1} - 1 \end{array} \right\} \text{ with rate } q^{c_i}. \end{aligned} \quad (57)$$

If a_i becomes zero, one deletes the domain a_i from the list of domains, and merges b_i and c_i with b_{i-1} and c_{i-1} , respectively.

To simulate the toy model efficiently, an algorithm suitable for rare event dynamics must be used due to the small rate of events [39]. In [23] an algorithm was employed that entails repeating the following steps.

- (i) List all possible events $\{n\}$ and assign to them rates $\{r_n\}$ according to the rules of the model.
- (ii) Choose an event m with probability r_m/R where $R = \sum_n r_n$.
- (iii) Advance time by $t \rightarrow t + \tau$, where $\tau = 1/R$.

The algorithm would be equivalent to a usual Monte Carlo simulation, where one time step is equivalent to one Monte Carlo sweep, if in step 3, τ were to be drawn from a Poisson distribution $R \exp[-R\tau]$. However, a saving in computer time can be had by making the approximation $\tau = 1/R$.

In [23] the dynamics were simulated for lattice sizes up to 9000. For simplicity we consider the case $N_A = N_B = N_C$. An example of typical behaviour of the average domain size is shown in figure 7. One can see that after an initial transient growth time the data fit very well with a $\ln t$ behaviour. (Note that the system size is large enough that the growth is N independent.) Simulations for different q values indicate that

$$\langle l \rangle = a \ln t / |\ln q| \quad (58)$$

with $a \simeq 2.6$. The toy model enables one to verify the scaling behaviour (58) and estimate the constant a . This would be very difficult to do by simulation of the full model (39).

One can further analyse the toy model by using an independent interval approximation as discussed in section 1.3. This was carried out in [23].

3.7. Generalization to $M \geq 3$ species

We now generalize the ABC model to M species where $M \geq 3$. We may define the most general M species model with nearest-neighbour particle exchanges that conserve the number

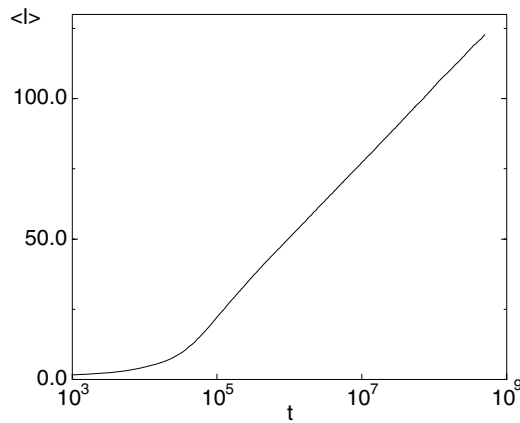
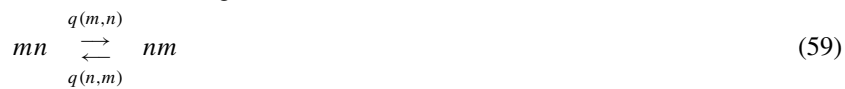


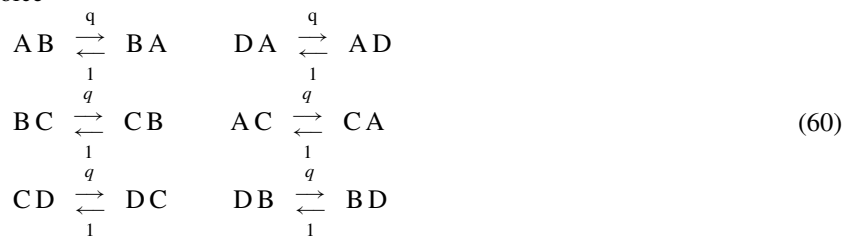
Figure 7. Monte Carlo simulation results for the toy model for the average domain size, $\langle l \rangle$, versus time, t , for $N = 9000$ and $q = 0.8$. The data is averaged over 1760 runs. There is clear evidence that $\langle l \rangle$ grows as $\ln t$ (figure taken from [23]).

of each species as follows. Let $X_i = 1, 2, \dots, M$ denote which type of particle is present at site i : $X_i = m$ means that site i is occupied by a particle of type m . Nearest-neighbour exchanges occur with the following rates:



and we take $q(m, m) = 1$. The model conserves N_m , the number of particles of type m , for all m .

According to the choice of the rates (59) the model may or may not phase separate. It is not difficult to choose rates so that phase separation does indeed occur. For example for $M = 4$ the choice



leads to phase separation into pure domains ordered ABCD. Generally, for $M > 3$ the structure of the metastable states can become quite complicated [23]. For example, domains ordered ACDACB are also metastable in the model defined by (60). We now find the conditions under which the dynamics (59) satisfy detailed balance with respect to a steady-state weight analogous to (41), (42):

$$W(\{X_i\}) = \text{const.} \times \prod_{i=1}^{N-1} \prod_{j=i+1}^N q(X_j, X_i) \tag{61}$$

where the constant is arbitrary.

Consider a particle exchange between sites k and $k + 1$, where $X_k = m$, $X_{k+1} = n$ and $k \neq N$. Expanding the product in (61), it is easy to verify that

$$\frac{W(X_1, \dots, m, n, \dots, X_N)}{W(X_1, \dots, n, m, \dots, X_N)} = \frac{q(n, m)}{q(m, n)}. \tag{62}$$

Since this holds for any m, n , and is irrespective of the number of particles of each species, the dynamics (59) satisfy detailed balance with respect to the weight (61) for all nearest-neighbour exchanges between sites k and $k+1$ with $k \neq N$. If the weights (61) are translationally invariant then detailed balance will also hold for exchanges between sites 1 and N .

Thus, to complete the proof of detailed balance it is sufficient to demand that (61) is translationally invariant. To do this we relabel sites $i \rightarrow i+1$. The weight then becomes

$$W(\{X_i\}) = \prod_{i=1}^{N-1} \prod_{j=i+1}^N q(X_{j-1}, X_{i-1}) \quad (63)$$

where X_0 is identical to X_N . Rewriting this equation by relabelling the indices we obtain

$$W(\{X_i\}) = \left[\prod_{i=1}^{N-1} \prod_{j=i+1}^N q(X_j, X_i) \right] \prod_{k=1}^{N-1} \frac{q(X_k, X_N)}{q(X_N, X_k)}. \quad (64)$$

Comparing (64) with (61) and noting for example that

$$\prod_{j=1}^N q(X_j, X_N) = \prod_{l=1}^M [q(l, X_N)]^{N_l} \quad (65)$$

one can see that (61) is translationally invariant if

$$\prod_{l=1}^M \left[\frac{q(m, l)}{q(l, m)} \right]^{N_l} = 1 \quad (66)$$

for every $m = 1, \dots, M$. Thus, detailed balance holds if (66) is satisfied.

In particular for the three-species model with particles labelled A B C the condition (66) becomes

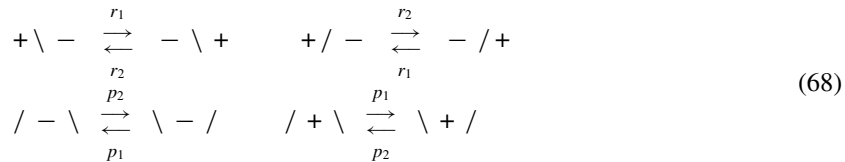
$$\begin{aligned} \left[\frac{q(A, B)}{q(B, A)} \right]^{N_B} \left[\frac{q(A, C)}{q(C, A)} \right]^{N_C} &= \left[\frac{q(B, A)}{q(A, B)} \right]^{N_A} \left[\frac{q(B, C)}{q(C, B)} \right]^{N_C} \\ &= \left[\frac{q(C, A)}{q(A, C)} \right]^{N_A} \left[\frac{q(C, B)}{q(B, C)} \right]^{N_B} = 1. \end{aligned} \quad (67)$$

The ABC model defined in section 3.2 has $\frac{q(B,A)}{q(A,B)} = \frac{q(C,B)}{q(B,C)} = \frac{q(A,C)}{q(C,A)} = q$ in which case (67) reduces to $N_A = N_B = N_C$.

The ABC model has been generalized to two dimensions [40] where the coarsening process generates striped domains perpendicular to the direction of the drive. The $\ln t$ growth of these domains is retained.

3.8. Other related models

A model closely related to the ABC model is that first introduced by Lahiri and Ramaswamy [41] in the context of sedimenting colloidal crystals. This model comprises two interpenetrating sublattices. On each sublattice there reside two species of particles with no holes. On the first sublattice (at integer sites) the particles are denoted by + and - whereas on the second sublattice (at half-integer sites) the particles are denoted as 'tilts' \ and /, for reasons that will become apparent below. The dynamics are defined as



i.e. the particles make nearest-neighbour exchanges on their respective sublattices but the rates are influenced by what kind of particle is occupying the intermediate site on the other sublattice. In [41] more general rates than (68) were originally considered but the above dynamics appear to capture all the generic behaviour [42, 43].

In the regime $r_1 > r_2$ and $p_1 > p_2$ phase separation is observed into ordered domains of $\setminus-$, $\setminus+$, $/+$, $/-$. That is, on each lattice the particles ultimately separate into pure domains with one ring rotated by $\pi/2$ with respect to the other. During the coarsening process domain lengths grow logarithmically in time. In [42] the separation into pure domains, as first analysed in the ABC model, was termed ‘strong phase separation’.

In the special case where each lattice is half filled with particles and

$$\frac{r_2}{r_1} = \frac{p_2}{p_1} \equiv q \tag{69}$$

(where the parameter q has been introduced to allow comparison with the ABC model), the steady state weight W_N satisfies detailed balance with respect to a long-range energy function very similar in form to (42):

$$W_N = Z_N^{-1} q^{\mathcal{H}} \tag{70}$$

where

$$\mathcal{H} = \frac{1}{2} \sum_{i=1}^N \sum_{j=1}^k \tau_{j-1/2} \sigma_i \tag{71}$$

and τ and σ are each Ising spins variables for one of the sublattices. $\sigma = +1(-1)$ corresponds to a $+$ ($-$) particle and $\tau = +1(-1)$ corresponds to tilt $/$ (\setminus).

A very useful intuitive picture of this energy function is to regard $\sum_{j=1}^k \tau_{j-1/2}$ as the height of an interface (relative to some origin) [42]. Thus the dynamics correspond to the $+$ and $-$ particles making nearest-neighbour interchanges on a landscape (implied by the tilt variables) that at the same time is evolving in a way coupled to the $+$, $-$ particles. The long-range energy corresponds to the gravitational potential energy of the $+$ particles on this landscape. A $+$ particle will have its energy minimized at the bottom of a valley of the interface. A ground state then corresponds to the configuration that allows the $+$ particles to minimize collectively their energy, namely, the tilt variables form one deep valley with the $+$ particles residing at the bottom:

$$-\setminus - \setminus - \setminus - \setminus + \setminus + \setminus + / + / + / + / + / - / - / - / .$$

The picture of particles moving on an evolving landscape is very appealing in the context of glassy dynamics. It is evocative of the glassy regime of a hard-sphere colloid where particles move in cages formed by the other particles—when a particle escapes from its cage it will cause the cages of other particles to be restructured.

In the regime $r_1 > r_2$ and $p_1 < p_2$ the system is in a disordered phase. In the regime $r_1 > r_2$ and $p_1 = p_2$ the fluctuations in the landscape are uncoupled to the particle dynamics, yet the system still exhibits an interesting coarsening dynamics [44].

A further model related to the ABC model has been studied by Arndt *et al* [45]. It was originally couched in terms of $+$, $-$ particles and holes diffusing on a one-dimensional periodic lattice with hop rates

$$\begin{aligned} + - &\xrightleftharpoons[q]{1} - + \\ + 0 &\xrightarrow{1} 0 + \\ 0 - &\xrightarrow{1} - 0. \end{aligned} \tag{72}$$

In order to make a comparison with the ABC model we identify a + particle with an A, a – particle with a B and a hole with a C; then the dynamics (72) become



Thus this model corresponds to the ABC model with some exchanges forbidden and for $q < 1$ one has the same strong phase separation. However for $q > 1$ this model enters a disordered phase, whereas in the ABC model one has phase separation but with the order of domains permuted to ACB. Originally it was thought that there was also a ‘mixed’ phase in the model [45]. It now appears that this is a very strong finite-size effect for $q \gtrsim 1$ [46]. An appealing feature of this model is that the steady state can, in principle, be computed exactly by a matrix product approach for all numbers of particles [45].

It should also be noted that a model with cyclic symmetry and nonconserving dynamics that exhibits coarsening has been studied [47].

4. Conclusions

In this paper I have reviewed a variety of simple models that exhibit anomalous coarsening in the sense that the dynamics slow down with time and the coarsening becomes anomalously slow—slower than the usual power law growth of domain size with time. In the models discussed the slowdown in the coarsening is due to dynamical constraints rather than any quenched disorder. The dynamical constraints imply that energy barriers must be surmounted in order for the system to coarsen further. Thus the system is delayed in metastable states for increasingly long times during the coarsening process and in this sense the evolution of the system is glassy.

In sections 2 and 3 I focused on two models: the ACIC and the ABC model. In the ACIC model the energy barriers encountered during coarsening are logarithmic in the domain size whereas for the ABC model the barriers are linear. This leads to the domain growth $\ell \sim t^{T \ln 2}$ (as $T \rightarrow 0$) for the ACIC and $\ell \sim \ln t$ for the ABC model. Despite similarities there are distinctions between the two models. For the ACIC the energy function is trivial—free spins in a field—and the dynamics obey detailed balance. But it is the existence of forbidden spin-flips that generates the energy barriers in the relaxation paths. On the other hand in the ABC model the dynamics are prescribed without regard to an energy function and no exchanges (that conserve the particle numbers) are forbidden. However in a special case one can identify an effective long-range energy function and the anomalous coarsening can be explained in terms of linear energy barriers in the coarsening process. Lastly, the ABC model will ultimately coarsen into pure domains whose size is related to the system size whereas the ACIC only coarsens up to a length $1/\epsilon$ that is independent of system size. For both models there exist other related models that exhibit similar behaviour, thus reinforcing their interest.

The question remains as to how faithfully the anomalous coarsening scenario describes a true (experimental) glassy system. Although the models are by no means meant to represent any particular system, one recovers the correct phenomenology—for example in the ACIC we derived stretched exponential decay of an auto-correlation function and EITS law for equilibration. Nevertheless it is widely thought that a coarsening system is distinct from a glassy system.

There are several reasons for this. Firstly, in a glassy system such as a hard-sphere colloid, the ordered phase (crystalline state) is thought to be irrelevant since its nucleation barrier is too large. Thus there are no coarsening domains of an ordered crystalline phase. On the other hand at present we do not have any known spatial order parameter for a glassy phase so it is unclear how domains of the glassy phase would coarsen. Secondly, coarsening implies a definite direction in the dynamics, towards the fully coarsened state. In contrast to this, phenomenological trap models of glassy dynamics [19] rely on a random exploration of the traps that exist in the phase space. That is, when a system manages to escape from one trap it falls randomly into another trap. In this way, as the timescale increases, the system will locate deeper traps and stay in them for longer. Finally, dynamically constrained models by nature rely on specific dynamics rather than the nature of an energy function (if it exists). This contrasts with the ‘inherent structures’ approach to glassy dynamics, where the energy landscape is the key feature [48, 49]. This point is examined in the present volume by Crisanti and Ritort.

Indeed a criterion has been proposed to distinguish between coarsening dynamics and glassy dynamics [50] in a microscopic model. One runs a simulation for a certain time then makes two copies of the simulation. These copies start from identical initial conditions (where the initial simulation was halted) but use different realizations of the noise in their dynamics, i.e. different sets of random numbers in a Monte Carlo simulation. Then, if the states of the two simulations remain strongly correlated (have a finite overlap) as time goes by one has a coarsening system. This is termed type I behaviour. On the other hand, if the states of the two simulations become less and less correlated then the system is a glassy system; this is termed type II behaviour. The idea behind this relies on the belief that for a coarsening system there is always a preferred direction in the phase space along which all simulations will be swept, whereas in a glassy system the traps in the phase space are essentially explored randomly by each simulation.

At present it is not clear how general this categorization is. For example it is not yet clear how systems that coarsen but have many ground states, such as the ABC model or the model of [42], are accounted for.

Let us also mention a 3d ferromagnetic Ising model with plaquette interactions [51]. In this model one has the usual doubly degenerate ferromagnetic ground states. In addition, flipping any plane of spins does not increase the energy. Thus in total there is an exponential number of degenerate ground states. In a quench to low temperature, type II glassy behaviour is exhibited [52], yet it is thought that coarsening occurs whereby a characteristic length grows anomalously slowly, possibly as $\ln t$. For a related model of competing ferromagnetic and next-nearest-neighbour antiferromagnetic interactions that has just the two ferromagnetic ground states, logarithmic coarsening is observed and explained in terms of energy barriers [21]. The glassy coarsening dynamics of the plaquette model is not so well understood [53]. It would certainly be of interest to broaden our understanding by studying further examples of anomalous coarsening.

Acknowledgments

It is a pleasure to thank my collaborators Yariv Kafri, Hari M Koduvvely, David Mukamel and Peter Sollich, with whom the work of sections 2 and 3 was carried out. I would also like to thank M Barma, R A Blythe, M E Cates, M Clincy, A Crisanti, D Das, S N Majumdar, F Ritort and A Rocco for stimulating discussions.

References

- [1] Angell C A 1995 *Science* **267** 1924
Ediger M D, Angell C A and Nagel S R 1996 *J. Phys. Chem.* **100** 13 201
Jäckle J 1986 *Rep. Prog. Phys.* **49** 171
- [2] Bouchaud J P, Cugliandolo L F, Kurchan J and Mézard M 1998 *Spin Glasses and Random Fields* ed A P Young (Singapore: World Scientific)
- [3] Adam G and Gibbs J H 1965 *J. Chem. Phys.* **43** 139
- [4] Richert R and Bässler H 1990 *J. Phys.: Condens. Matter* **2** 2273
- [5] Palmer R G, Stein D L, Abrahams E and Anderson P W 1984 *Phys. Rev. Lett.* **53** 958
- [6] Fredrickson G H and Anderson H C 1984 *Phys. Rev. Lett.* **53** 1244
- [7] Schulz M and Trimper S 1999 *J. Stat. Phys.* **94** 173
- [8] Pitts S J, Young T and Andersen H C 2000 *J. Chem. Phys.* **113** 8671
- [9] Jäckle J and Eisinger S 1991 *Z. Phys. B* **84** 115
- [10] Eisinger S and Jäckle J 1993 *J. Stat. Phys.* **73** 643
- [11] Reiter J, Mauch F and Jäckle J 1992 *Physica A* **184** 458
- [12] Muñoz M A, Gabrielli A, Inaoka H and Pietronero L 1998 *Phys. Rev. E* **57** 4354
- [13] Mauch F and Jäckle J 1999 *Physica A* **262** 98
- [14] Sollich P and Evans M R 1999 *Phys. Rev. Lett.* **83** 3238
- [15] Ritort F 1995 *Phys. Rev. Lett.* **75** 1190
- [16] Kirkpatrick T R and Thirumalai D 1987 *Phys. Rev. B* **36** 5388
Kirkpatrick T R and Wolynes P 1987 *Phys. Rev. A* **35** 3072
- [17] Bouchaud J P and Mézard M 1994 *J. Physique I* **4** 1109
- [18] Marinari E, Parisi G and Ritort F 1994 *J. Phys. A: Math. Gen.* **27** 7615
- [19] Bouchaud J P 1992 *J. Physique I* **2** 1705
Bouchaud J P and Dean D S 1995 *J. Physique I* **5** 265
Bouchaud J P, Comtet A and Monthus C 1995 *J. Physique I* **5** 1521
- [20] Vilgis T A 1990 *J. Phys.: Condens. Matter* **2** 3667
- [21] Shore J D, Holtzer M and Sethna J P 1992 *Phys. Rev. B* **46** 11 376
- [22] Bray A J 1994 *Adv. Phys.* **43** 357
- [23] Evans M R, Kafri Y, Koduvvely H M and Mukamel D 1998 *Phys. Rev. Lett.* **80** 425
Evans M R, Kafri Y, Koduvvely H M and Mukamel D 1998 *Phys. Rev. E* **58** 2764
- [24] Doering C R and ben-Avraham D 1988 *Phys. Rev. A* **38** 3035
ben-Avraham D 1997 *Nonequilibrium Statistical Mechanics in One Dimension* (Cambridge: Cambridge University Press) ch 2
- [25] Krapivsky P L and Ben-Naim E 1997 *Phys. Rev. E* **56** 3788
- [26] Derrida B, Godrèche C and Yekutieli I 1991 *Phys. Rev. A* **44** 6241
- [27] Bray A J, Derrida B and Godrèche C 1994 *Europhys. Lett.* **27** 175
Rutenberg A D and Bray A J 1994 *Phys. Rev. E* **50** 1900
- [28] For a review see Schmittmann B and Zia R K P 1995 *Statistical mechanics of driven diffusive systems Phase Transitions and Critical Phenomena* vol 17, ed C Domb and J L Lebowitz (London: Academic)
- [29] Mukamel D 2000 *Soft and Fragile Matter: Nonequilibrium Dynamics, Metastability and Flow* ed M E Cates and M R Evans (Bristol: Institute of Physics Publishing) (cond-mat/0003424) and references therein
- [30] Evans M R 2000 *Braz. J. Phys.* **30** 42 (cond-mat/0007293) and references therein
- [31] Privman V (ed) 1997 *Nonequilibrium Statistical Mechanics in One Dimension* (Cambridge: Cambridge University Press)
- [32] Sollich P and Evans M R, unpublished
- [33] Newman M E J and Moore C 1999 *Phys. Rev. E* **60** 5068
Garrahan J P and Newman M E J 2000 *Phys. Rev. E* **62** 7670
- [34] Buhot A and Garrahan J P 2001 *Phys. Rev. E* **64** 021505
- [35] Majumdar S N, Dean D S and Grassberger P 2001 *Phys. Rev. Lett.* **86** 2301
- [36] Landau L D and Lifshitz E M 1980 *Statistical Physics* vol 1 (New York: Pergamon)
- [37] O'Loan O J, Evans M R and Cates M E 1998 *Phys. Rev. E* **58** 1404
- [38] Andrews G E 1976 *The theory of partitions Encyclopedia of Mathematics and its Applications* vol 2 (Reading, MA: Addison-Wesley)
- [39] Bortz A B, Kalos M H and Lebowitz J L 1975 *J. Comput. Phys.* **17** 10
- [40] Kafri Y, Biron D, Evans M R and Mukamel D 2000 *Eur. Phys. J. B* **16** 669
- [41] Lahiri R and Ramaswamy S 1997 *Phys. Rev. Lett.* **79** 1150

- [42] Lahiri R, Barma M and Ramaswamy S 2000 *Phys. Rev. E* **61** 1648
- [43] Ramaswamy S, Barma M, Das D and Basu A 2001 *Preprint cond-mat/0103062*
- [44] Das D and Barma M 2000 *Phys. Rev. Lett.* **85** 1602
- [45] Arndt P F, Heinzl T and Rittenberg V 1998 *J. Phys. A: Math. Gen.* **31** L45
Arndt P F, Heinzl T and Rittenberg V 1999 *J. Stat. Phys.* **97** 1
- [46] Rajewsky N, Sasamoto T and Speer E R 2000 *Physica A* **279** 123
- [47] Frachebourg L, Krapivsky P L and Ben-Naim E 1996 *Phys. Rev. E* **54** 6186
- [48] Stillinger F H and Weber T A 1984 *Science* **225** 983
Stillinger F H 1995 *Science* **267** 1935
- [49] Crisanti A, Ritort F, Rocco A and Sellito M 2000 *J. Chem. Phys.* **113** 10615
- [50] Barrat A, Burioni R and Mézard M 1996 *J. Phys. A: Math. Gen.* **29** 1311
- [51] Lipowski A 1997 *J. Phys. A: Math. Gen.* **30** 7365
Lipowski A and Johnston D 2000 *J. Phys. A: Math. Gen.* **33** 4451
- [52] Swift M R, Bokil H, Travasso R D M and Bray A J 2000 *Phys. Rev. B* **62** 11494
- [53] Lipowski A, Johnston D and Espriu D 2000 *Phys. Rev. E* **62** 3404
Lipowski A and Johnston D 2001 *Preprint cond-mat/0106211*
- [54] Garrahan 2001 *J. Phys.: Condens. Matter* at press
- [55] Buhot 2001 *J. Phys.: Condens. Matter* at press